Hydrology and
Earth System
Sciences

Open Access

EGU

Supplement of

Constructing a geography of heavy-tailed flood distributions: insights from common streamflow dynamics

Hsing-Jui Wang et al.

Correspondence to: Hsing-Jui Wang (hsjwang@gmail.com)

Contents of this supplement

Introduction

This supporting information comprises one text, five figures, and one table. Section S1 introduces the statistical method employed and discusses the results depicted in Figure S1. Figure S1 illustrates the comparison between the estimated recession exponent and flood tail behavior using both the constant time step method (CTS) and the exponential time step method (ETS). Figure S2 presents a plot of the event-based analysis of hydrograph recession exponents. Figure S3 depicts a schematic diagram outlining the hydrograph recession analysis utilized in this study. Figure S4 displays the comparison of sample sizes of identified tails of empirical distributions based on Kolmogorov-Smirnov and Anderson-Darling tests. Figure S5 showcases L-moment diagrams of all case studies. Table S1 provides the adopted criteria for Köppen climate classification (adapted from Beck et al., 2018).

S1. The comparison of using the constant time step (CTS) and exponential time step (ETS) methods in estimating hydrograph recession exponents for inferring flood tail behavior.

We compare the estimated recession exponent based on both the constant time step method (CTS, currently adopted in this study) and the exponential time step method (ETS) in Figure S1. In panel a, the results are categorized into four quadrants based on the characteristic tail behavior (i.e., heavy tails if recession exponents > 2 and nonheavy tails if recession exponents < 2).

Panel b illustrates the proportion of case studies in terms of consistent (I+III), inconsistent 1 (II), and inconsistent 2 (IV) using the CTS compared to the ETS method. Notably, the results demonstrate consistent tail behavior identified using both CTS and ETS, with 90% of case studies exhibiting the same behavior. A minimal fraction (0.1%) shows heavy tails based on ETS but non-heavy tails based on CTS (II), while a limited fraction (9.9%) exhibits the opposite pattern (IV).

Panel c presents a pie chart depicting the relative distribution of bias cases within each Köppen climate group to explore whether bias cases are concentrated in specific climate areas. For one

single Köppen group i, the normalized bias ratio (b_i) is calculated based on the case number of bias (n_i), the total number of cases in that specific Köppen group (N_i), and normalized by the sum of bias ratios for all Köppen groups (B):

$$b_i = \left(\frac{n_i}{N_i}\right) \cdot \left(\frac{1}{B}\right) \quad , \quad B = \sum \left(\frac{n_i}{N_i}\right)$$

$$i \in \{Csa, BSh, Dsb, Cfb, Csb, BSk, Dfb, Cfa, Dfa, Dfc, BWk, ET\}$$

The results reveal that potential biases are widespread across most climate groups (10 out of 12), showing no apparent distinctions among them.
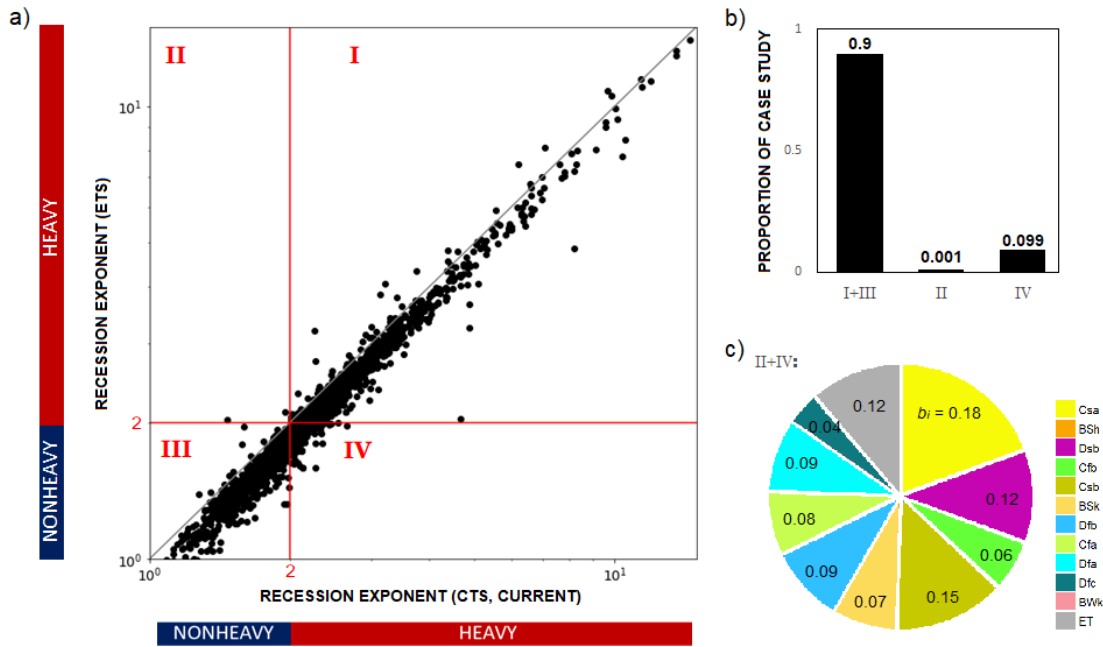

Figure S1. The comparison between the estimated recession exponent and flood tail behavior based on the constant time step method (CTS) and the exponential time step method (ETS). The recession exponents are estimated using both Constant Time Step (CTS) and Exponential Time Step (ETS) methods (Roques et al., 2017), with the maximum interval for derivative computation set to one-third of the identified recession length for the latter. The analysis is computed for all 1997 case studies based on daily discharge. (a) The distribution of estimated exponents categorized by flood tail quadrant using a critical value of two (Wang et al., 2023). (b) The proportion of case studies in three categories: consistent tail behavior (quadrants I and III), inconsistent tail behavior quadrant II (nonheavy tails based on CTS but heavy tails based on ETS) and quadrant IV (heavy tails based on CTS but nonheavy tails based on ETS). (c) The relative contribution (b_i, detailed in supporting information Section S1) of Köppen climate groups covered in this study to case studies in quadrants II and IV.
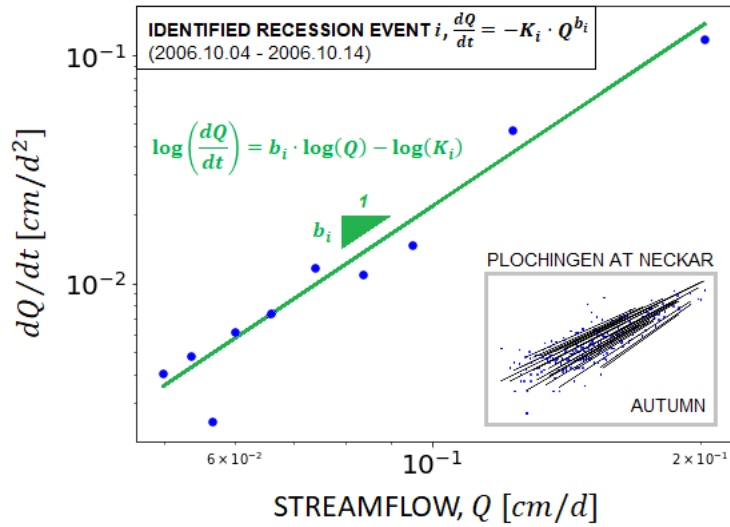
Figure S2. An exemplary plot illustrating the event-based analysis of hydrograph recession exponents. The case studies from the autumn period of the Plochingen at the River Neckar, Germany, are presented.
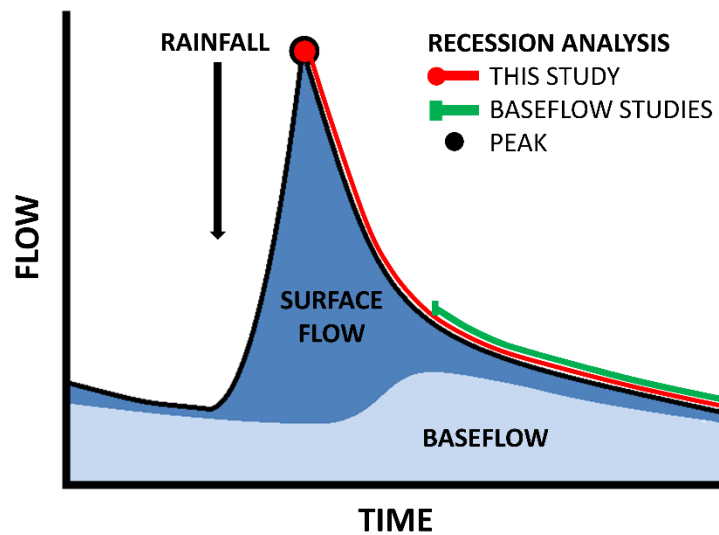
Figure S3. A schematic diagram of hydrograph recession analysis adopted in this study. Adapted from Mathai and Mujumdar (2022).
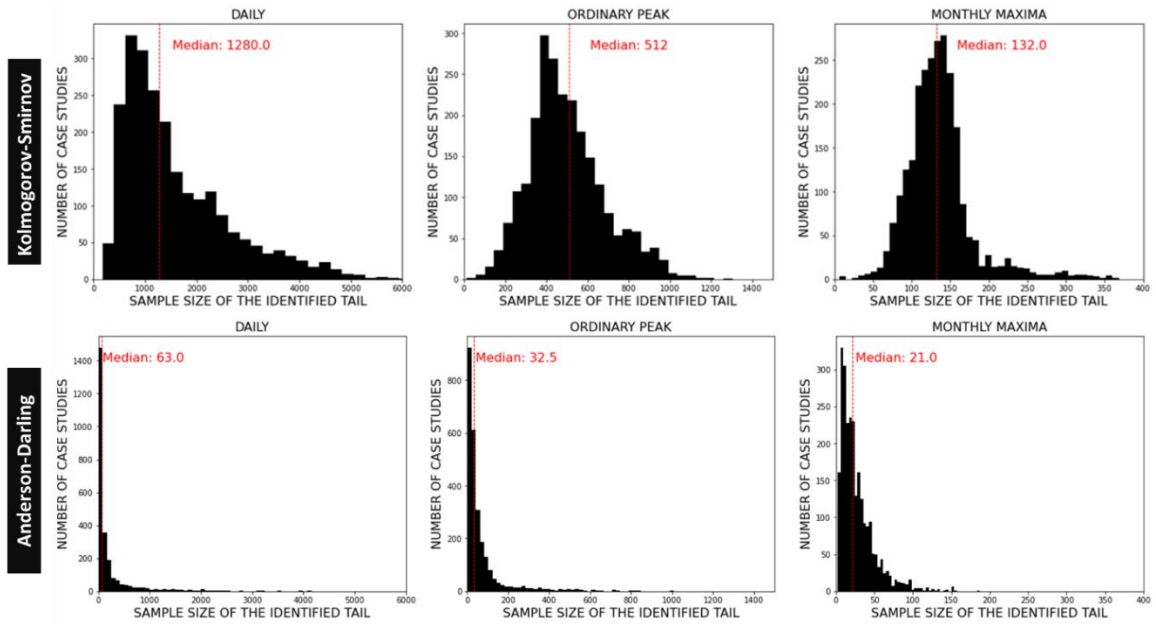
Figure S4. Sample sizes of the identified tail of empirical distributions based on Kolmogorov-Smirnov and Anderson-Darling tests.
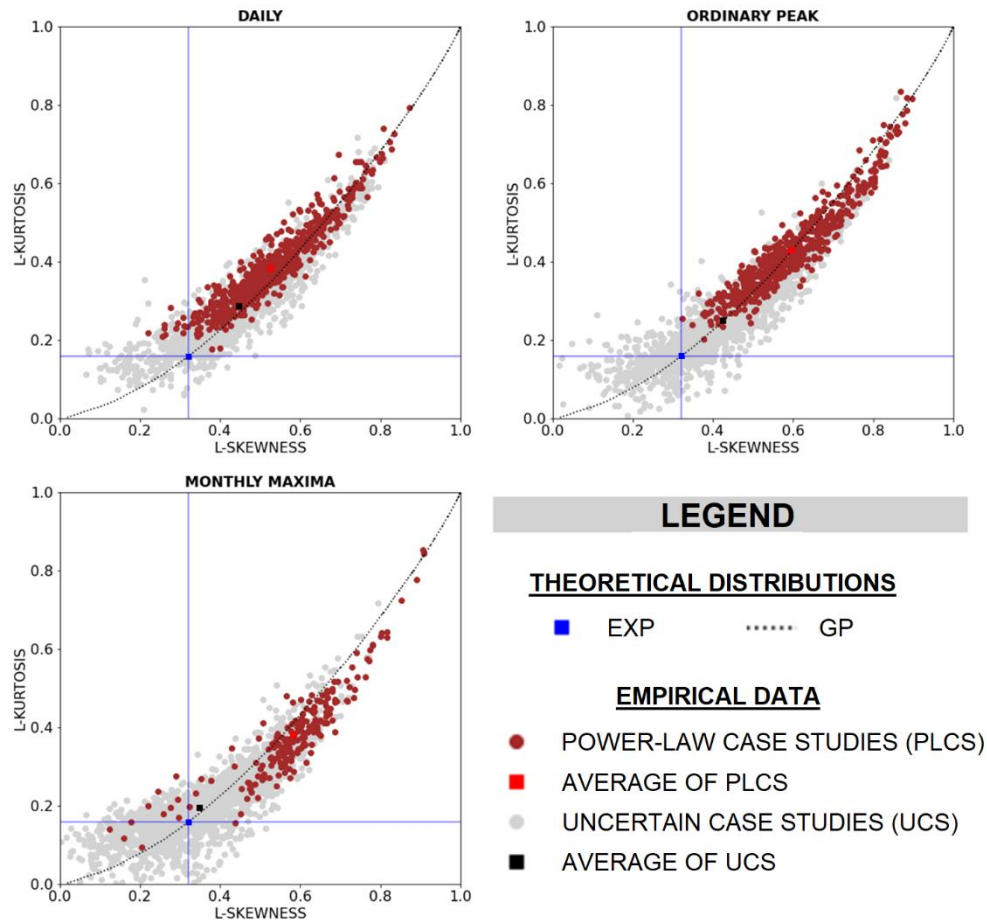
Figure S5. L-moment diagram with empirical L-moment ratios of (a) daily streamflow, (b) ordinary peaks, and (c) monthly maxima of all case studies. Red dots indicate the power-law-tailed case studies (PLCS) whereas gray dots denote those uncertain case studies (UCS), based on the categorization of Figure 2. The red (black) square represents the average empirical L-moment ratios of power-law-tailed (uncertain) case studies. Theoretical L-moment ratios of exponential (EXP, blue square) and Generalized Pareto (GP) distributions are provided for reference. The former is commonly regarded as the differentiation between heavy- and non-heavy-tailed distributions (Merz et al., 2022), whereas the latter are recognized for exhibiting power law decay in extreme behaviors. 97.8%, 100%, and 94.1% of PLCS in the analyses of daily, ordinary peaks, and monthly maxima, respectively, have greater L-skewness and L-kurtosis (blue line) than the exponential distribution.

Table S1. The adopted criterion of Köppen climate classification (adapted from Beck et al., 2018). Classes covered by this study are highlighted with gray shading.

1st	2nd	3rd	DESCRIPTION	QUANTITATIVE CRITERION[a]
A			Tropical	$Not\ [B]\ \&\ T_{cold} \geq 18$
	f		• Rainforest	$P_{dry} \geq 60$
	m		• Monsoon	$Not\ [Af]\ \&\ P_{dry} \geq (100 - \frac{MAP}{25})$
	w		• Savannah	$Not\ [Af]\ \&\ P_{dry} < (100 - \frac{MAP}{25})$
B			Arid	$MAP < 10 \times P_{threshold}$
	W		• Desert	$MAP < 5 \times P_{threshold}$
	S		• Steppe	$MAP \geq 5 \times P_{threshold}$
		h	• Hot	$MAT \geq 18$
		k	• Cold	$MAT < 18$
C			Temperate	$Not\ [B]\ \&\ T_{hot} > 10\ \&\ 0 < T_{cold} < 18$
	s		• Dry summer	$P_{sdry} < 40\ \&\ P_{sdry} < \frac{P_{wwet}}{3}$
	w		• Dry winter	$P_{wdry} < \frac{P_{swet}}{10}$
	f		• Without dry season	$Not\ [Cs]\ nor\ [Cw]$
		a	• Hot summer	$T_{hot} \geq 22$
		b	• Warm summer	$Not\ [a]\ \&\ T_{mon10} \geq 4$
		c	• Cold summer	$Not\ [a\ or\ b]\ \&\ 1 \leq T_{mon10} < 4$
D			Cold	$Not\ [B]\ \&\ T_{hot} > 10\ \&\ T_{cold} \leq 0$
	s		• Dry summer	$P_{sdry} < 40\ \&\ P_{sdry} < \frac{P_{wwet}}{3}$
	w		• Dry winter	$P_{wdry} < \frac{P_{swet}}{10}$
	f		• Without dry season	$Not\ [Ds]\ nor\ [Dw]$
		a	• Hot summer	$T_{hot} \geq 22$
		b	• Warm summer	$Not\ [a]\ \&\ T_{mon10} \geq 4$
		c	• Cold summer	$Not\ [a, b,\ or\ d]$
		d	• Very cold winter	$Not\ [a\ or\ b]\ \&\ T_{cold} < -38$
E			Polar	$Not\ [B]\ \&\ T_{hot} \leq 10$
	T		• Tundra	$T_{hot} > 0$
	F		• Frost	$T_{hot} \leq 0$

[a]Variable definitions: MAT, mean annual air temperature (°C); T_{cold}, the air temperature of the coldest month (°C); T_{hot}, the air temperature of the warmest month (°C); T_{mon10}, the number of months with air temperature >10 °C (unitless); MAP, mean annual precipitation (mm y^{-1}); P_{dry}, precipitation in the driest month (mm month^{-1}); P_{sdry}, precipitation in the driest month in summer (mm month^{-1}); P_{wdry}, precipitation in the driest month in winter (mm month^{-1}); P_{swet}, precipitation in the wettest month in summer (mm month^{-1}); P_{wwet}, precipitation in the wettest month in winter (mm month^{-1}); $P_{threshold} = 2 \times MAT$ if >70% of precipitation falls in winter, $P_{threshold} = 2 \times MAT + 28$ if >70% of precipitation falls in summer, otherwise $P_{threshold} = 2 \times MAT + 14$. Summer (winter) is the six-month period that is warmer (colder) between April-September and October-March.